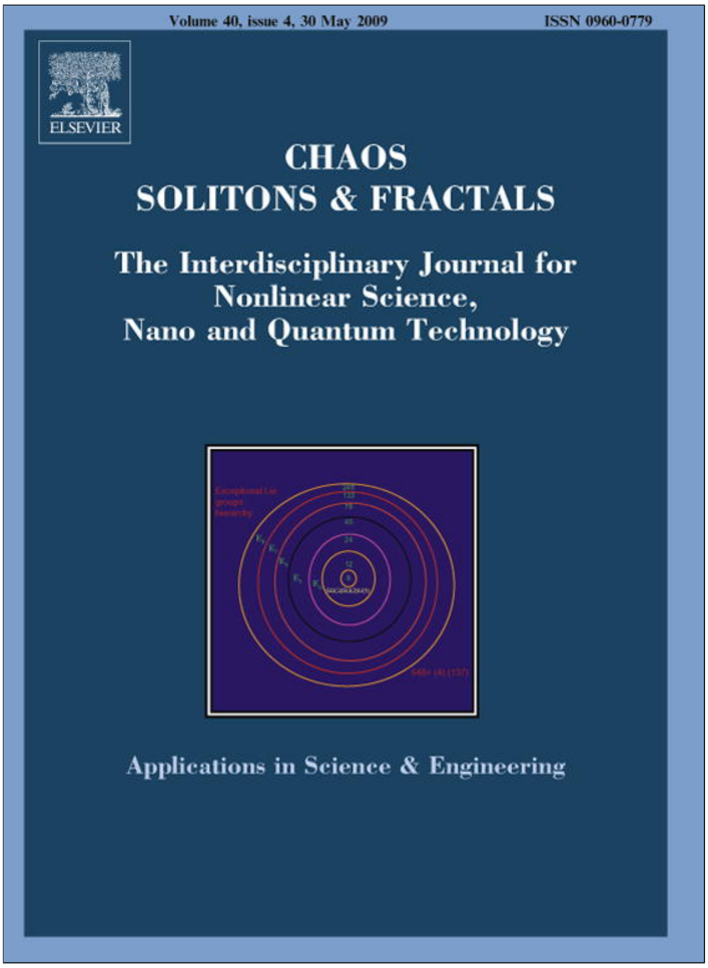
Volume 40, issue 4, 30 May 2009
ISSN 0960-0779
ELSEVIER
CHAOS
SOLITONS & FRACTALS
The Interdisciplinary Journal for
Nonlinear Science,
Nano and Quantum Technology
Applications in Science & Engineering

Available online at www.sciencedirect.com

ScienceDirect

Chaos, Solitons and Fractals 40 (2009) 1637–1652

CHAOS
SOLITONS & FRACTALS

www.elsevier.com/locate/chaos

Chaos and its control in the pitch motion of an asymmetric magnetic spacecraft in polar elliptic orbit

Manuel Iñarrea

Universidad de La Rioja, Área de Física Aplicada, 26006 Logroño, Spain

Accepted 11 September 2007

Abstract

We study the pitch attitude dynamics of an asymmetric magnetic spacecraft in a polar almost circular orbit under the influence of a gravity gradient torque. The spacecraft is perturbed by the small eccentricity of the elliptic orbit and by a small magnetic torque generated by the interaction between the Earth's magnetic field and the magnetic moment of the spacecraft. Under both perturbations, we show that the pitch motion exhibits heteroclinic chaotic behavior by means of the Melnikov method. Numerical methods applied to simulations of the pitch motion also confirm the chaotic character of the spacecraft attitude dynamics. Finally, a linear time-delay feedback method for controlling chaos is applied to the governing equations of the spacecraft pitch motion in order to remove the chaotic character of initially irregular attitude motions and transform them into periodic ones.

1. Introduction

The dynamics of a rotating body has been a classic topic of study in mechanics. So, in the XVIII and XIX centuries, several aspects of the motion of a rotating rigid body were studied by many authors such as Euler, Cauchy, Jacobi, Poinsot, Lagrange and Kovalevskaya. However, the study of the dynamics of rotating bodies is still very important in modern science. From a theoretical point of view, this topic offers quite interesting models and problems in the field of non-linear dynamics. Moreover, during the last decades, the interest in the dynamics of rotating bodies has considerably increased in astrodynamics and space engineering because it is an useful model to study, at first approximation, the attitude dynamics of spacecrafts [20,51].

Any spacecraft in orbit is under the action of several kinds of external disturbance torques as the solar radiation pressure, the gravity gradient torque, the magnetic torque caused by the Earth's magnetic field, or the aerodynamic drag torque. Although all these external disturbances are not large in comparison with the weight of the vehicle, they can not be considered as negligible in a closer study of the attitude dynamics of a spacecraft because their influence may be significant in the real attitude motion of the vehicle. Sometimes, these external torques can be considered as perturbations with undesirable effects on the attitude motion of the spacecraft, as they may generate chaotic behaviors. Nevertheless,

E-mail address: manuel.inarrea@unirioja.es

0960-0779/$ - see front matter
doi:10.1016/j.chaos.2007.09.047

it is important to note that, from other point of view, these torques can also be considered in a positive way, exploiting their effects as control methods over the spacecraft attitude with the goal of stabilizing chaotic orientation motions.

The gravity gradient torque results from the variation in the gravitational force over the distributed mass of the spacecraft. This torque is related to one of the more interesting aspect in the attitude dynamics of a spacecraft: the so-called pitch motion [20]. An asymmetric satellite in closed orbit around the Earth tends to ride with its longest axis vertical due to the effect of the gravity gradient torque. If it is deviated from this equilibrium position, the satellite would oscillate or rotate about that attitude. This kind of oscillation is sometimes called librations. During the second part of the last century, the topic of the effects of the gravity gradient torque was studied in relation to the determination of the spacecrafts motions. Klemperer and Baker [28], Schindler [50] and Klemperer [29], studied the librations of dumbbell and ellipsoid of revolution satellites in circular orbit. On the other hand, Moran [40] analyzed the effects of the planar librations on the orbital motion of an asymmetric spacecraft. Modi and Brereton [38,39] investigated the libration periodic solutions of a gravity-gradient oriented satellite in circular and elliptic orbit.

The magnetic torque is generated by the interaction between the possible magnetic features of the spacecraft and the magnetic field of the Earth. These magnetic features may arise from both internal electric currents and spacecraft materials subject to induced or permanent magnetization. The cases of the Vanguard I and Tiros I satellites can be cited as representative examples of the effects of magnetics torques on the attitude motion of spacecrafts [20,41]. The strength of the magnetic torque depends on the intrinsic magnetic moment of the spacecraft, but it is usually smaller than a tenth part of the gravity gradient torque [5,20].

Data obtained from the flight experience of different satellites launched during the aerospace history show that unexpected behaviors have arisen in the attitude motion of several spacecrafts. These undesirable orientation motions have been frequently due to the action of those external torques which had not been taken into account in the spacecraft design [41–43]. Therefore, these unexpected behaviors move to study, analyze and understand, from a theoretic point of view, the attitude motion of spacecrafts in different conditions, in order to detect in advance and prevent undesirable orientation motions. During last decades, numerous theoretic studies have pointed out the existence of chaotic attitude behaviors in several kinds of satellites under the action of different perturbations. In this way, Tong and Rimrott [56] have numerically investigated the planar libration of an asymmetric satellite in elliptic orbit under the gravity gradient torque. Teofilatto and Graziani [55] have studied the same system but considering the three-dimensional libration motion of the spacecraft. Holmes and Marsden [19], Koiller [30], and Peng and Liu [47] have analyzed free gyrostats with a slightly asymmetric rotor. Karasopoulos and Richardson [26,27] have studied analytically and numerically the attitude dynamics of a satellite under the gravity gradient torque. Nixon and Misra [44] and Fujii and Ichiki [11] have investigated numerically the orientation motion of tethers. Tong et al. [57] have also treated the case of an asymmetric gyrostat under the uniform gravitational field. Meehan and Asokanthan [35] and Gray et al. [16] have studied the attitude motion of satellites with internal dissipation of energy. Beletsky et al. [2] have treated numerically the case of a magnetic spacecraft in circular polar orbit subject only to the torque generated by the geomagnetic field. Lanchares et al. [33] and Iñarrea et al. [21–23] have investigated analytically and numerically the chaotic orientation motions of several kinds of asymmetric spacecrafts with time-dependent moments of inertia in different external conditions. In many of these studies, the authors have applied the Melnikov method [37], which proves to be a powerful analytical tool to determine, at first order, the existence of homo/heteroclinic intersections and so chaotic behavior in near-integrable systems.

In this paper, we study the pitch attitude dynamics of an asymmetric magnetic spacecraft in a polar almost circular orbit under the influence of a gravity gradient torque. The spacecraft is perturbed by the small eccentricity of the elliptic orbit and by a small magnetic torque generated by the interaction between the Earth's magnetic field and the magnetic moment of the spacecraft. In this, work we have also made use of the Melnikov method to analyzed if our perturbed spacecraft exhibits heteroclinic chaotic attitude motions. It is important to note that, due to the change in the orientation of the spacecraft in its pitch motion, the center of gravity of the satellite does not coincide, in general, with its mass center. Therefore, there is a coupling between the orbital and the libration motion of the spacecraft. However, as the vehicle is small compared to its distance to the mass center of the Earth, the deviations of the center of gravity of the spacecraft from its mass center may be considered very small. So, we also assume that there is no coupling between the orbital and pitch motion, hence the orbit of the spacecraft around the Earth is not affected by the libration motion.

As it has been theoretically shown and proved in real experience, many spacecraft systems in different conditions may exhibit chaotic or unstable behaviors. Therefore, this kind of dynamical systems represents a suitable field for the applications of control methods. During last years, new control techniques have been developed to be applied to nonlinear dynamical systems in order to transform chaotic or unstable behaviors into regular or periodic motions [4]. These new techniques have a goal: to achieve the control of chaos, that is, the possibility of bringing order into chaos. Some investigations have been undertaken using control schemes with and without feedback. However, the feedback control methods became a distinguished and important group among the plethora of different control techniques.

Probably, the reason should be found in the advantage that they offer: they need comparatively small perturbations to get the control of the system, with respect to the non-feedback schemes (see [49]).

Several time delayed feedback control methods have been recently applied to stabilize different dynamical systems by various authors [6,25,34,46,53]. One of the simplest of these time delayed control techniques was first proposed by Pyragas [48] in order to synchronize the current state of a system and a time delayed version of itself. Taking this delayed time as the period of an unstable periodic orbit such a control scheme can be used to stabilize the orbit. This method of control is usually named time-delayed autosynchronization or TDAS. Two important advantages of this method are related with the feedback used: it does not requires rapid switching or sampling, nor does it require a reference signal corresponding to the desired orbit. This technique has been improved in [52,3] using a more elaborated feedback: the extended time-delayed autosynchronization or ETDAS, where TDAS appears as a limiting case.

Control schemes based on feedback methods have been utilized in orbital and attitude dynamics of spacecrafts. In this way, Ge et al. [13], have applied a delay feedback control method, among other ones, to remove chaos in the motion of a gyrostat satellite in absence of external torques. Tsui and Jones [58] have compared the relative efficacy of three control techniques, one of them time-delay feedback, in the chaotic attitude of a rigid satellite with thrusters and generic perturbations. Fujii and co-workers [12] have investigated the application of a time-delay feedback method in order to get the stabilization of the libration motion of a rigid satellite in elliptic orbit. El-Gohary and Youssif [7,8] have considered the optimal feedback control law to stabilize the equilibrium positions of a rotating rigid body using internal rotors. Meehan and Asokanthan [36] have analyzed the chaos removal in the attitude of a gyrostat satellite with internal dumping by means of a feedback control method based on the action of a external torque. Peláez and Lorenzini [46] and Iñarrea and Peláez [24] have studied the application of different feedback control techniques to transform unstable periodic orbits into asymptotically stable ones in the attitude dynamics of an electrodynamic tether.

The present paper is structured in the following way. In Section 2, we describe in detail the perturbed system and we also express the equation of motion of the spacecraft pitch motion. Then we point out the main features of the phase space of the unperturbed system. In Section 3 we calculate the Melnikov function of the perturbed spacecraft. In Section 4 by means of computer numerical simulations of the spacecraft pitch motion we use several numerical techniques to check the validity of the analytical result obtained through the Melnikov method. Poincaré surface of sections reveal us the persistence of periodic pitch motions in the perturbed system with the same period of the orbital motion. In Section 5, we apply the ETDAS control method to the governing equations of motion in order to transform initially chaotic pitch motions into one of the persistent periodic ones.

2. Description of the system and equations of motion

Let us consider an asymmetric magnetic spacecraft in a polar almost circular orbit in the gravitational and magnetic fields of the Earth. The spacecraft has its own magnetic moment generated by permanent magnets or electric current loops. The magnetic field of the Earth is modeled as a perfect dipole aligned with the Earth's rotation axis. We focus the analysis on the system attitude dynamic and we neglect any decay or raise in the orbit followed by the spacecraft.

We make use of three different right oriented orthonormal reference frames:

- The inertial geocentric frame $\mathscr{E}\{O_{\mathrm{E}}, X_{\mathrm{E}}, Y_{\mathrm{E}}, Z_{\mathrm{E}}\}$ with the origin O_{E} at the center of mass of the Earth, the $X_{\mathrm{E}}Y_{\mathrm{E}}$ plane coincident with the equatorial plane, the X_{E} axis passing through the ascending node N, and the Z_{E} axis aligned with the Earth's rotation axis.
- The orbital frame $\mathscr{R}\{O, X, Y, Z\}$ with origin O at the mass center of the spacecraft, the Z axis along the local vertical pointing to the mass center of the Earth O_{E}, the Y axis is normal to the orbital plane and the X axis is in the orbital plane but it does not coincides exactly with the velocity vector of the spacecraft due to the eccentricity of the orbit. The base vectors of $\mathscr{R}$ are $\vec{r}_1, \vec{r}_2, \vec{r}_3$. See Fig. 1. In the usual aircraft and spacecraft terminology, the X, Y, Z axes are called respectively *roll*, *pitch* and *yaw* axes [51,20].
- The body frame $\mathscr{B}\{O, x, y, z\}$, is established with the directions of the axes coincident with the principal axes of the spacecraft. The base vectors of $\mathscr{B}$ are $\vec{b}_1, \vec{b}_2, \vec{b}_3$.

As it is well known, the relative orientation between two of these three reference frames results by means of three consecutive rotations involving the Euler angles (ψ, θ, ϕ). To move from the orbital axes $\{X, Y, Z\}$ to the body axes $\{x, y, z\}$, the first rotation is about the Z axis through an angle ψ (yaw). The second rotation is about the new axis Y' by an angle θ (pitch). Finally, the third rotation is about the new axis x through an angle ϕ (roll), reaching the body axes $\{x, y, z\}$ (see Fig. 2). This particular set of Euler angles are commonly used in aircraft and spacecraft attitude and

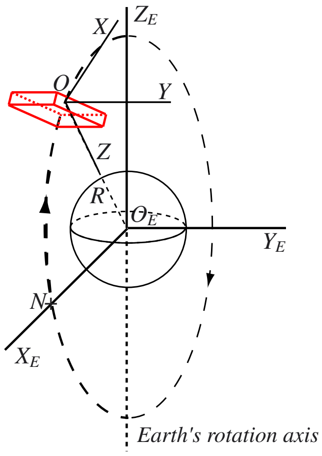

Fig. 1. The inertial geocentric frame $\mathscr{E}$ and the orbital reference frame $\mathscr{R}$.

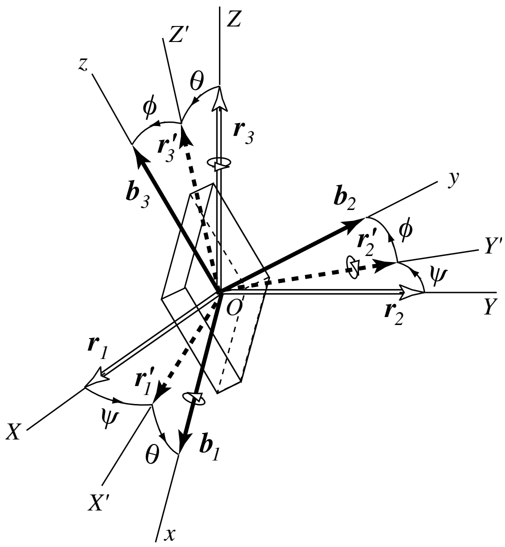

Fig. 2. The three consecutive rotations from the orbital frame $\mathscr{R}$ to the body frame $\mathscr{B}$ through the Euler yaw, pitch and roll angles (ψ, θ, ϕ).

are also known as Tait-Bryan or Cardan angles [20,59,18]. We do not make use of the classical Euler angles [14] because they have a singularity in the particular orientation that is studied in this paper.

Without control, two kind of forces are acting upon the magnetic spacecraft: the gravitational interaction and the magnetic one. Therefore, the attitude dynamics of the spacecraft is governed by two torques: (i) the one provided by the gravity gradient and (ii) the magnetic torque generated by the interaction between the magnetic moment of the spacecraft and the Earth's magnetic field. Taking into account these torques, the classical theorem of angular momentum about the mass center O of the spacecraft, expressed in the inertial geocentric frame $\mathscr{E}$, is

$$\frac{\mathrm{d}\vec{G}}{\mathrm{d}t} = \vec{N}_{\mathrm{g}} + \vec{N}_{\mathrm{m}},$$

where $\vec{G}$ is the angular momentum of the spacecraft, $\vec{N}_{\mathrm{g}}$ is the gravitational torque, and $\vec{N}_{\mathrm{m}}$ the magnetic one. This equation can be also expressed in the non-inertial body frame $\mathscr{B}$ as

$$\frac{\mathrm{d}'\vec{G}}{\mathrm{d}t} + \vec{\omega}_{\mathrm{T}} \times \vec{G} = \vec{N}_{\mathrm{g}} + \vec{N}_{\mathrm{m}},$$

where $\vec{\omega}_{\mathrm{T}}$ is the total angular velocity of the spacecraft, and the prime in the derivative stands for it is calculated in the body frame $\mathscr{B}$.

In this frame $\mathscr{B}$, the angular momentum $\vec{G}$ can be written as $\vec{G} = \mathbb{I}\vec{\omega}_{\mathrm{T}}$, where $\mathbb{I}$ is the tensor of inertia of the spacecraft. As it is expressed in the body frame $\mathscr{B}$ of the principal axes of the spacecraft, this tensor is a diagonal one, that is, $\mathbb{I} = \mathrm{diag}(I_x, I_y, I_z)$, where I_x, I_y and I_z are the moments of inertia of the spacecraft. We assume an asymmetric spacecraft with this specific relation $I_x > I_y > I_z$. In this way, the theorem of the angular momentum takes the form

$$\mathbb{I}\frac{\mathrm{d}\vec{\omega}_{\mathrm{T}}}{\mathrm{d}t} + \vec{\omega}_{\mathrm{T}} \times \mathbb{I}\vec{\omega}_{\mathrm{T}} = \vec{N}_{\mathrm{g}} + \vec{N}_{\mathrm{m}}, \tag{1}$$

where the prime is dropped because it is not necessary to distinguish between the temporal derivatives calculated in one frame or the other.

Taking into account that in the total angular velocity ω_{T} of the spacecraft there are two contributions: one from the orbital motion and other form the attitude one, thus this total angular velocity ω_{T} can be written in the body frame $\mathscr{B}$ as

$$\vec{\omega}_{\mathrm{T}} = \vec{\omega} + C_{\mathscr{R}\mathscr{B}}\vec{\omega}_{\mathrm{o}} = \omega_x\vec{b}_1 + \omega_y\vec{b}_2 + \omega_z\vec{b}_3 + C_{\mathscr{R}\mathscr{B}}(-\dot{v}\vec{r}_2). \tag{2}$$

Here $\vec{\omega} = \omega_x\vec{b}_1 + \omega_y\vec{b}_2 + \omega_z\vec{b}_3$ is the attitude angular velocity of the body about its mass center O in the body frame $\mathscr{B}$. Besides, $\vec{\omega}_{\mathrm{o}} = -\dot{v}\vec{r}_2$ is the orbital angular velocity of the spacecraft expressed in the orbital frame $\mathscr{R}$, where v is the true anomaly that gives us the angular position of the spacecraft in its orbit. Finally, $C_{\mathscr{R}\mathscr{B}}$ is the transformation matrix from the orbital frame $\mathscr{R}$ to the body frame $\mathscr{B}$, that is, the matrix of the three consecutive rotations involving the Euler angles (ψ, θ, ϕ).

As it is well known, the components $(\omega_x, \omega_y, \omega_z)$ of the angular velocity $\vec{\omega}$ in the body frame $\mathscr{B}$, can be written in terms of the Euler angles (ψ, θ, ϕ) and their velocities $(\dot{\psi}, \dot{\theta}, \dot{\phi})$ as [59,51,18,20]

$$\begin{cases} \omega_x = \dot{\phi} - \dot{\psi}\sin\theta, \\ \omega_y = \dot{\theta}\cos\phi + \dot{\psi}\cos\theta\sin\phi, \\ \omega_z = \dot{\psi}\cos\theta\cos\phi - \dot{\theta}\sin\phi. \end{cases} \tag{3}$$

Due to the gravity gradient and the finite dimension of the spacecraft, it is under the action of a gravitational torque $\vec{N}_{\mathrm{g}}$ about the body mass center O. The components of this torque $\vec{N}_{\mathrm{g}}$ in the body frame $\mathscr{B}$ are given by [59,51,20]:

$$\begin{cases} N_{gx} = \frac{3\mu_{\mathrm{g}}}{R^3}(I_z - I_y)\sin\phi\cos\phi\cos^2\theta, \\ N_{gy} = \frac{3\mu_{\mathrm{g}}}{R^3}(I_z - I_x)\cos\phi\sin\theta\cos\theta, \\ N_{gz} = \frac{3\mu_{\mathrm{g}}}{R^3}(I_x - I_y)\sin\phi\sin\theta\cos\theta, \end{cases} \tag{4}$$

where $\mu_{\mathrm{g}} = Gm_e = 3.986 \times 10^{14}\ \mathrm{N\ m^2/kg}$ is the mass parameter of the Earth, and R is the distance between the mass centers of the spacecraft and Earth.

As we consider that the spacecraft has its own magnetic moment, it is also under the action of another torque generated by the interaction with the Earth's magnetic field. We suppose that the terrestrial magnetic field $\vec{B}$ is generated by a perfect dipole located at the mass center of the Earth and aligned with its rotation axis [59,51,20]. In this way, the components of the magnetic field $\vec{B} = B_x\vec{r}_1 + B_y\vec{r}_2 + B_z\vec{r}_3$ are expressed in the orbital frame $\mathscr{R}$ in IS units as

$$\begin{cases} B_x = \frac{\mu_{\mathrm{o}}}{4\pi}\frac{\mu_m}{R^3}\sin i\cos(v + \Omega), \\ B_y = -\frac{\mu_{\mathrm{o}}}{4\pi}\frac{\mu_m}{R^3}\cos i, \\ B_z = \frac{\mu_{\mathrm{o}}}{4\pi}\frac{\mu_m}{R^3}2\sin i\sin(v + \Omega), \end{cases} \tag{5}$$

where μ_{o} is the magnetic permeability of free space, $\mu_m \approx 7.8 \times 10^{22} A \cdot m$ is the geomagnetic dipole moment [31], i and Ω are the inclination and the argument of perigee of the spacecraft orbit respectively.

The magnetic torque $\vec{N}_{\mathrm{m}}$ acting over the spacecraft, calculated in the body frame $\mathscr{B}$, is given by the cross product,

$$\vec{N}_{\mathrm{m}} = \vec{M} \times C_{\mathscr{R}\mathscr{B}}\vec{B} = (M_x\vec{b}_1 + M_y\vec{b}_2 + M_z\vec{b}_3) \times C_{\mathscr{R}\mathscr{B}}(B_x\vec{r}_1 + B_y\vec{r}_2 + B_z\vec{r}_3), \tag{6}$$

where $\vec{M} = M_x\vec{b}_1 + M_y\vec{b}_2 + M_z\vec{b}_3$ is the own magnetic moment of the spacecraft expressed in the body frame $\mathscr{B}$, the components (B_x, B_y, B_z) are those of Eq. (5), and $C_{\mathscr{R}\mathscr{B}}$ is the transformation matrix from the orbital frame $\mathscr{R}$ to the body frame $\mathscr{B}$.

Making use of Eqs. (2)–(6) the equation of motion (1) could be explicitly written in terms of the Euler angles (ψ, θ, ϕ), their velocities $(\dot{\psi}, \dot{\theta}, \dot{\phi})$ and their accelerations $(\ddot{\psi}, \ddot{\theta}, \ddot{\phi})$, resulting in quite cumbersome expressions.

Nevertheless, in this paper we adopt the following assumptions: (i) the spacecraft is tracing a polar orbit, that is, its inclination is $i = \pi/2$; (ii) the magnetic moment $\vec{M}$ of the spacecraft keeps constant and aligned with the principal axis z of the spacecraft, that is, $\vec{M} = (0, 0, M)$ in the body frame $\mathscr{B}$; and (iii) the roll and yaw motions are initially quiescent, that is, $\psi(0) = \dot{\psi}(0) = 0$ and $\phi(0) = \dot{\phi}(0) = 0$. Under all these assumptions, the equations of the attitude motion become

$$\begin{cases} \frac{\mathrm{d}^2\psi}{\mathrm{d}t^2} = 0, \\ \frac{\mathrm{d}^2\theta}{\mathrm{d}t^2} = \frac{\mathrm{d}^2 v}{\mathrm{d}t^2} - \frac{3\mu_\mathrm{g}(I_x - I_z)}{I_y R^3}\sin\theta\cos\theta + \frac{\mu_\mathrm{o} M \mu_\mathrm{m}}{4\pi I_y R^3}[\cos\theta\cos(v+\Omega) - 2\sin\theta\sin(v+\Omega)], \\ \frac{\mathrm{d}^2\phi}{\mathrm{d}t^2} = 0, \end{cases}$$

Therefore, in this situation, roll and yaw motions are not excited by the pitch one. The direction of the principal axis y of the spacecraft is fixed in space and it is always normal to the orbital plane. The orientation of the spacecraft can be described with only one angle θ, the pitch one. And there is only one non–trivial equation of motion for the attitude dynamics of the system.

Now it is convenient to replace the time t by the true anomaly v as the independent variable of the problem. In this change of variable, we make use of the following equations

$$R = \frac{p}{1 + e\cos v} \quad \frac{\mathrm{d}v}{\mathrm{d}t} = \frac{\sqrt{\mu_\mathrm{g} p}}{R^2},$$

where e is the eccentricity and $p = a(1 - e^2)$ is the parameter of the orbit traced by the spacecraft. By means of the chain rule, we obtain the following equation for the pitch motion,

$$\ddot{\theta} = -\frac{3(I_x - I_z)}{I_y}\frac{\sin\theta\cos\theta}{1 + e\cos v} + \frac{2e\sin v}{1 + e\cos v}(\dot{\theta} - 1) + \frac{\mu_\mathrm{o} M \mu_\mathrm{m}}{4\pi\mu_\mathrm{g} I_y}\frac{[\cos\theta\cos(v+\Omega) - 2\sin\theta\sin(v+\Omega)]}{1 + e\cos v},$$

where v is the independent variable. From this equation and along the rest of the paper, the dot means derivation with respect to the true anomaly v. In this equation, the last term comes from the interaction with the Earth's magnetic field, whereas the other terms arise from the gravity gradient and inertial Coriolis forces.

Now, by introducing the following new dimensionless parameters

$$K = \frac{3(I_x - I_z)}{I_y}, \quad \beta = \frac{\mu_\mathrm{o} M \mu_\mathrm{m}}{4\pi\mu_\mathrm{g} I_y},$$

we obtain

$$\ddot{\theta} = -\frac{K\sin\theta\cos\theta}{1 + e\cos v} + \frac{2e\sin v}{1 + e\cos v}(\dot{\theta} - 1) + \beta\frac{[\cos\theta\cos(v+\Omega) - 2\sin\theta\sin(v+\Omega)]}{1 + e\cos v}.$$

Therefore, the attitude dynamics of the spacecraft depends basically on three parameters: K which describes the spacecraft's asymmetry, the orbit eccentricity e, and β which describes the strength of the magnetic interaction.

As we consider that the spacecraft is tracing an almost circular orbit, and also we assume that the magnetic interaction is much weaker than the gravitational one, in this case we can suppose that both parameters e and β are small, that is, $e \ll 1$ and $\beta \ll 1$. Hence, making use of the expansion $(1 + e\cos v)^{-1} \approx 1 - e\cos v$, and omitting terms of second order in the small parameters e and β, the equation of the pitch motion results in

$$\ddot{\theta} = -K\sin\theta\cos\theta + Ke\cos v\sin\theta\cos\theta + 2e\sin v(\dot{\theta} - 1) + \beta[\cos\theta\cos(v+\Omega) - 2\sin\theta\sin(v+\Omega)]. \tag{7}$$

The terms in e and β in this equation can be considered as small perturbations. In this way, the unperturbed system ($e = \beta = 0$) coincides with an asymmetric spacecraft in circular orbit under only the gravity gradient torque. Thus, the equation of motion of the unperturbed spacecraft is given by

$$\ddot{\theta} = -K\sin\theta\cos\theta.$$

This equation may be rewritten in form of a system of two differential equations of first order as

$$\begin{cases} \dot{\theta} = \omega = f_1, \\ \dot{\omega} = -K\sin\theta\cos\theta = f_2. \end{cases} \tag{8}$$

These differential equations correspond to the following Hamiltonian

$$\mathscr{H} = \frac{1}{2}p_\theta^2 + \frac{K}{2}\sin^2\theta,$$

with $p_\theta = \omega$. In this case, the Hamilton function coincides with the sum of the rotational kinetic energy of the spacecraft about its mass center, plus the gravity gradient potential energy of the body. As it can be seen, the unperturbed spacecraft is one degree of freedom and, therefore, it is an integrable system.

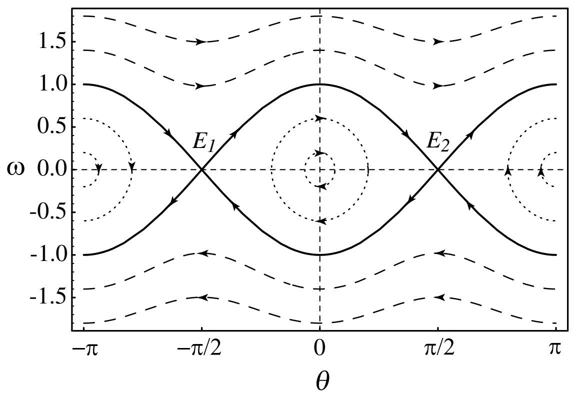

Fig. 3. The phase space of the unperturbed pitch motion of an asymmetric spacecraft in circular orbit under the gravity gradient torque for $K = 1$.

Eqs. (8) are those corresponding to a nonlinear pendulum taking 2θ as the angular variable. Therefore, it is known that the system has unstable equilibria at $(\theta,\omega) = (\pm(2n+1)\pi/2, 0)$, and stable equilibria at $(\pm n\pi, 0)$. The Fig. 3 shows the main features of the phase flow for the unperturbed system (8) for $K = 1$. The two unstable equilibria, denoted by E_1 and E_2, are connected by four heteroclinic trajectories. These orbits are the separatrices of the phase space, the thick continuous lines in that figure.

The energy of the system corresponding to the unstable equilibria and the separatrices is $\mathscr{E}_{\mathrm{sep}} = K/2$. These separatrices divide the phase space in two different classes of the pitch motion. On the one hand, oscillations, the dotted lines inside the separatrices, when the energy of the spacecraft is $\mathscr{E} < \mathscr{E}_{\mathrm{sep}}$,

$$\begin{cases} \theta = \arcsin\left[\frac{1}{k}\,\mathrm{sn}\left(\sqrt{K}v, \frac{1}{k}\right)\right], \\ \omega = \sqrt{2\mathscr{E}}\,\mathrm{cn}\left(\sqrt{K}v, \frac{1}{k}\right), \end{cases} \quad k^2 = \frac{K}{2\mathscr{E}} \tag{9}$$

which are periodic with period $T = \mathscr{K}(1/k)/\sqrt{K}$, being $\mathscr{K}$ the complete integral of first kind. On the other hand, tumbling rotations, the dashed lines outside the separatrices, when the energy of the spacecraft is $\mathscr{E} > \mathscr{E}_{\mathrm{sep}}$,

$$\begin{cases} \theta = \arcsin\left[\mathrm{sn}\left(\sqrt{2\mathscr{E}}v, k\right)\right], \\ \omega = \sqrt{2\mathscr{E}}\,\mathrm{d}n\left(\sqrt{2\mathscr{E}}v, k\right), \end{cases} \quad k^2 = \frac{K}{2\mathscr{E}} \tag{10}$$

which are periodic with period $T = \mathscr{K}(k)/\sqrt{2\mathscr{E}}$. Besides, the solutions corresponding to the four asymptotic heteroclinic trajectories, are

$$[\theta^{\pm}(v), \omega^{\pm}(v)] = \{\pm \arcsin\left[\tanh\left(\sqrt{K}v\right)\right],\ \pm\sqrt{K}\ \mathrm{sech}\left(\sqrt{K}v\right)\}, \tag{11}$$

subject to the initial conditions $(\theta_{\mathrm{o}}^{\pm}(0), \omega_{\mathrm{o}}^{\pm}(0)) = \left(0, \pm\sqrt{K}\right)$. The four heteroclinic trajectories form the stable $W_{\mathrm{s}}(E_1)$, $W_{\mathrm{s}}(E_2)$ and unstable $W_{\mathrm{u}}(E_1)$, $W_{\mathrm{u}}(E_2)$ manifolds corresponding to the two unstable equilibria, that join smoothly together. So it holds that $W_{\mathrm{s}}(E_1) = W_{\mathrm{u}}(E_2)$ and $W_{\mathrm{u}}(E_1) = W_{\mathrm{s}}(E_2)$.

3. Chaotic pitch motion: the Melnikov function

Let us consider the perturbed system. Now the stable and unstable manifolds are not forced to coincide and it is possible that they intersect transversally in the corresponding Poincaré surface of section, leading to an infinite number of new heteroclinic points. Then, a heteroclinic tangle is generated. In such a case, because of the perturbations, the pitch motion of the spacecraft near the unperturbed separatrices becomes extremely complicated and chaotic in the sense that the system exhibits Smale's horseshoes and a stochastic layer appears near the unperturbed separatrices. Inside this chaotic layer small isolated regions of regular motion with periodic orbits can also appear.

The existence of heteroclinic intersections may be proved, at first order, by means of the Melnikov method [17]. In order to apply the Melnikov method, the Eq. (7) can be expressed as the following system of two differential equations of first order

$$\begin{cases} \dot{\theta} = \omega = f_1 + g_1, \\ \dot{\omega} = -K\sin\theta\cos\theta + Ke\cos v\sin\theta\cos\theta + 2e\sin v(\omega - 1) + \beta[\cos\theta\cos(v+\Omega) - 2\sin\theta\sin(v+\Omega)] = f_2 + g_2, \end{cases} \tag{12}$$

where $g_1 = 0$ and $g_2 = Ke\cos v\sin\theta\cos\theta + 2e\sin v(\omega - 1) + \beta[\cos\theta\cos(v+\Omega) - 2\sin\theta\sin(v+\Omega)]$.

The Melnikov function, $M^{\pm}(v_0)$, for the system (12) is given by

$$\begin{aligned} M^{\pm}(v_0) &= \int_{-\infty}^{\infty} \vec{f}[\vec{z}^{\pm}(v)] \wedge \vec{g}[\vec{z}^{\pm}(v), v + v_0]\mathrm{d}v = \int_{-\infty}^{\infty} \{f_1[\vec{z}^{\pm}(v)]g_2[\vec{z}^{\pm}(v), v+v_0] - f_2[\vec{z}^{\pm}(v)]g_1[\vec{z}^{\pm}(v), v+v_0]\}\,\mathrm{d}v \\ &= \int_{-\infty}^{\infty} f_1[\vec{z}^{\pm}(v)]g_2[\vec{z}^{\pm}(v), v+v_0]\mathrm{d}v \\ &= \int_{-\infty}^{\infty} \omega^{\pm}(v)\{Ke\cos(v+v_0)\sin\theta^{\pm}(v)\cos\theta^{\pm}(v) + 2e\sin(v+v_0)(\omega^{\pm}(v) - 1) + \beta[\cos\theta^{\pm}(v)\cos(v+v_0 \\ &\quad + \Omega) - 2\sin\theta^{\pm}(v)\sin(v+v_0+\Omega)]\}\mathrm{d}v, \end{aligned} \tag{13}$$

where $\vec{z}^{\pm}(v) = (\theta^{\pm}(v), \omega^{\pm}(v))$ are precisely the solutions of the unperturbed heteroclinic orbits (11).

The Melnikov function $M^{\pm}(v_0)$ give us a measure of the distance between the stable and unstable manifolds of the perturbed hyperbolic fixed points. Thus, if $M^{\pm}(v_0)$ has simple zeroes, there are transverse intersections between the stable and unstable manifolds in the corresponding Poincaré surface of section.

Now, by substitution of Eqs. (11) into (13) we obtain, for the positive branch of the Melnikov function,

$$\begin{aligned} M(v_0) &= M_1 + M_2 + M_3 \\ &= K^{3/2}e\int_{-\infty}^{\infty}\left[\mathrm{sech}^2\left(\sqrt{K}v\right)\tanh\left(\sqrt{K}v\right)\cos(v+v_0)\right]\mathrm{d}v + 2e\sqrt{K} \\ &\quad\times\int_{-\infty}^{\infty}\left[\mathrm{sech}\left(\sqrt{K}v\right)\left[\sqrt{K}\mathrm{sech}\left(\sqrt{K}v\right) - 1\right]\sin(v+v_0)\right]\mathrm{d}v + \beta\sqrt{K} \\ &\quad\times\int_{-\infty}^{\infty}\left[\mathrm{sech}^2\left(\sqrt{K}v\right)\cos(v+v_0+\Omega) - 2\frac{\sinh\left(\sqrt{K}v\right)}{\cosh^2\left(\sqrt{K}v\right)}\sin(v+v_0+\Omega)\right]\mathrm{d}v \end{aligned} \tag{14}$$

being M_1 and M_2 the Melnikov function corresponding to the perturbation coming from the elliptic orbit, and M_3 the one arising from the magnetic interaction.

These three integrals, M_1, M_2 and M_3 can be calculated integrating them by parts and arriving at other simpler integral tabulated in [15]. In this way, we obtain

$$\begin{aligned} M_1 &= -\frac{\pi e}{2}\mathrm{cosech}\left(\frac{\pi}{2\sqrt{K}}\right)\sin(v_0), \\ M_2 &= 2\pi e\left[\mathrm{cosech}\left(\frac{\pi}{2\sqrt{K}}\right) - \mathrm{sech}\left(\frac{\pi}{2\sqrt{K}}\right)\right]\sin(v_0), \\ M_3 &= \frac{\pi\beta}{\sqrt{K}}\left[\mathrm{cosech}\left(\frac{\pi}{2\sqrt{K}}\right) - 2\mathrm{sech}\left(\frac{\pi}{2\sqrt{K}}\right)\right]\cos(v_0+\Omega). \end{aligned} \tag{15}$$

Thus, the complete Melnikov function $M(v_0)$ results in

$$M(v_0) = C_1\sin(v_0) + C_2\cos(v_0+\Omega), \tag{16}$$

where the coefficients C_1 and C_2, which depends on the system parameters K, e and β, are given by

$$\begin{aligned} C_1(K,e) &= \pi e\left[\frac{3}{2}\mathrm{cosech}\left(\frac{\pi}{2\sqrt{K}}\right) - 2\mathrm{sech}\left(\frac{\pi}{2\sqrt{K}}\right)\right], \\ C_2(K,\beta) &= \frac{\pi\beta}{\sqrt{K}}\left[\mathrm{cosech}\left(\frac{\pi}{2\sqrt{K}}\right) - 2\mathrm{sech}\left(\frac{\pi}{2\sqrt{K}}\right)\right]. \end{aligned} \tag{17}$$

Therefore, as the coefficients C_1 and C_2 vanish for different values of parameter K, we can conclude from Eq. (16) that the Melnikov function $M(v_0)$ of the perturbed spacecraft has simple zeroes. Hence, both perturbations produce heteroclinic intersections between the stable and unstable manifolds of the hyperbolic equilibria E_1 and E_2 in the corresponding Poincaré surface of section. Therefore the perturbed spacecraft shows chaotic pitch motions near the unperturbed separatrices.

4. Numerical analyses

In order to check the validity of the analytical result given by the Melnikov method, we have made use of several numerical techniques. They are based on the numerical integration of the equations of motion (12) by means of a Runge–Kutta algorithm of fifth order with fixed step [32].

Firstly, we have numerically calculated the stable $W_s(E_i)$ and unstable $W_u(E_i)$ manifolds associated to the saddle fixed points E_1, E_2 of the Poincaré map. The Poincaré surface of section consist of sections $v = \text{cte} \cdot (\text{mod}2\pi)$ of the three–dimensional (θ, ω, v) extended phase space. This computation has been carried out by means of the commercial software DYNAMICS [45]. Fig. 4a shows the invariant manifolds of the unstable equilibria E_1 in the perturbed spacecraft with $K = 1$ and $e = \beta = 0.1$. Fig. 4b shows the same for the other unstable equilibria E_2. For shake of clarity we show the four invariant manifolds in two different graphs. The unstable manifolds are depicted as darker lines, whereas the stable ones are depicted as clearer lines. As it can be seen clearly in both figures, the stable and unstable manifolds of each equilibria transversally intersect each other in many heteroclinic points. This numerical calculation confirms the analytical results provided by the Melnikov method: the perturbations of our system generate the intersections between the invariant manifolds, and therefore the arising of chaotic behavior in the pitch motion of the spacecraft.

In order to visualize the effect of the perturbations in the pitch motion dynamics of the spacecraft, we have studied the time histories of the pitch angle θ, the trajectories of the system in the reduced phase space (θ, ω), the $v = 2\pi$ Poincaré surfaces of section, and the power spectra of several trajectories. To this end, we have used appropriate algorithms [54,9] implemented with the symbolic manipulator MATHEMATICA [60].

Fig. 5 shows the numerical simulations of the same trajectory with initial conditions near to the unperturbed separatrix $(\theta_o, \omega_o) = (1.39412, 0)$ for the unperturbed spacecraft (left column), and for the perturbed spacecraft with $(K = 1$, $e = 0.03$ and $\beta = 0.02$ (right column). For these initial conditions, in absence of perturbations, the pitch motion corresponds with a periodic oscillation with the positive z axis of the spacecraft pointing to Earth. Moreover, this periodic oscillation has a period twice the orbital period 2π, as only two points appear in the Poincaré surface of section (c), and a sharp isolated peak stands out at frequency $f = 0.5$ in the flat power spectrum (d). In this figure, we can see clearly how this periodic pitch motion in the unperturbed system becomes a chaotic one when the perturbations go into action. This transformation is confirmed in the right column by the irregular time evolution of pitch angle θ (a) which turns into a complex trajectory in the reduced phase space (b) where oscillations and tumbling rotations alternate in a random order. The Poincaré map (c) also shows how this motion appear as a cloud of disordered points located at a

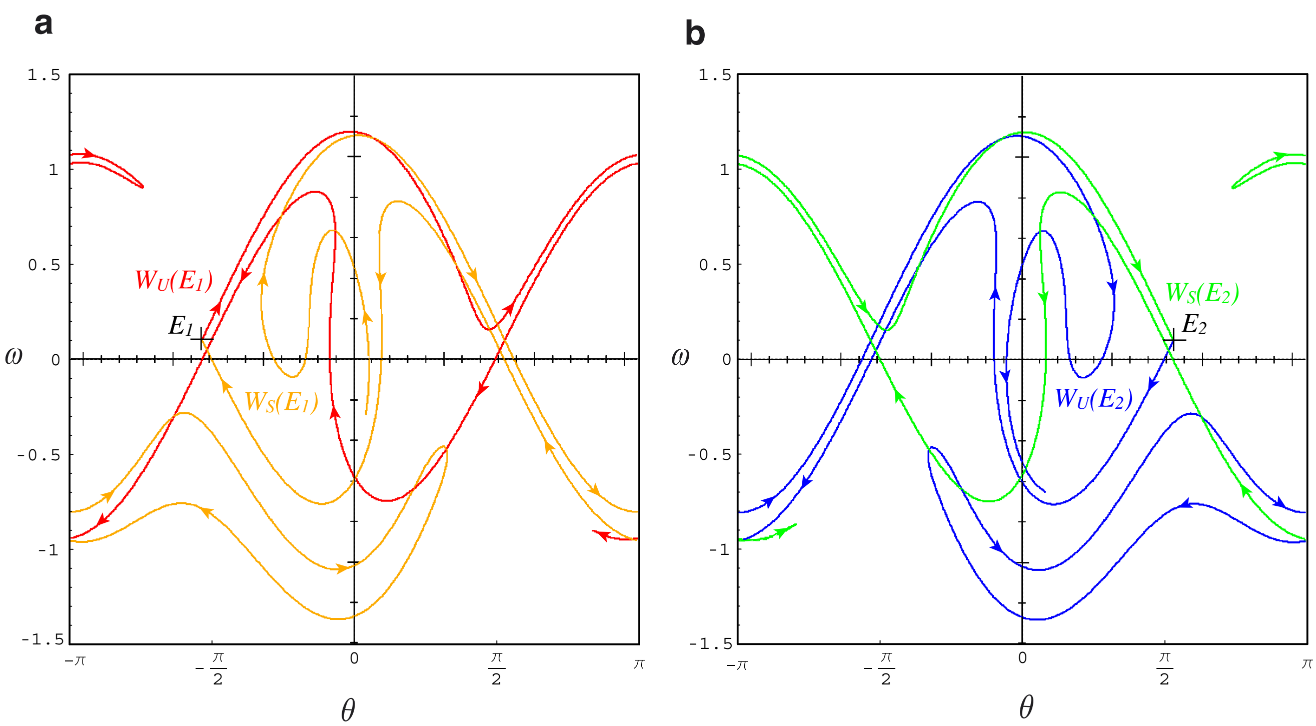

Fig. 4. Heteroclinic intersections of the invariant manifolds of the equilibria E_1 (a) and E_2 (b) in the $v = 2\pi$ Poincaré map for $K = 1$ and $e = \beta = 0.1$.

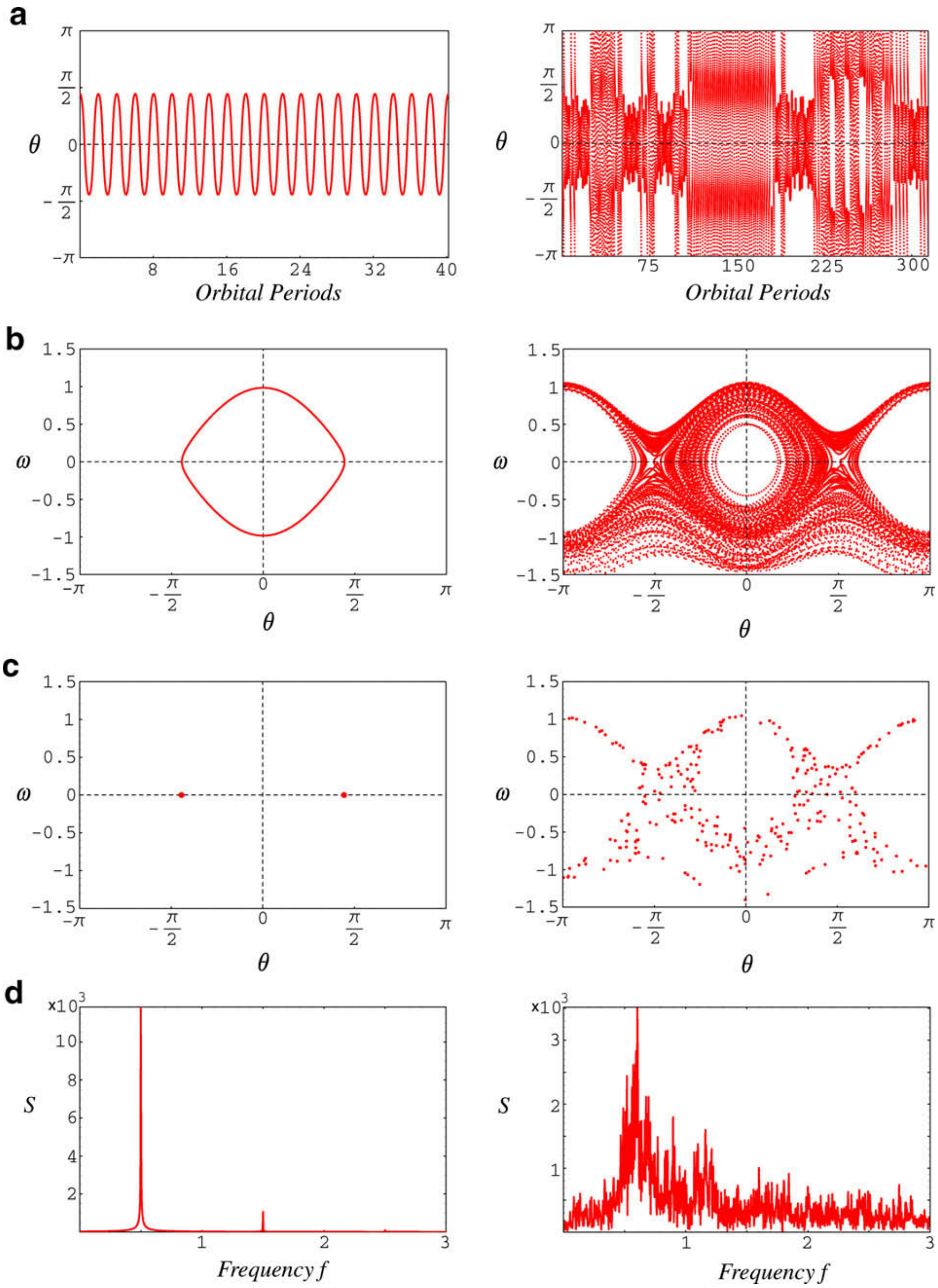

Fig. 5. Numerical simulation of the pitch motion for initial conditions near the unperturbed separatrix $(\theta_o, \omega_o) = (1.39412, 0)$. Left column: unperturbed spacecraft $(K = 1, e = \beta = 0)$. Right column: perturbed spacecraft $(K = 1, e = 0.03, \beta = 0.02)$. (a) Time evolution of angle θ. (b) Trajectory in the phase space. (c) $v = 2\pi$ Poincaré surface of section. (d) Power spectrum.

stochastic layer around the unperturbed separatrix. Finally, the broadly distributed power spectrum (d) gives another sign of the chaotic behavior of the pitch motion.

It is important to note that, not all the regular pitch motions of the unperturbed spacecraft become into chaotic ones when the perturbations go into action. Despite of the perturbations, some periodic pitch motions persist with the same period as the orbital motion, that is, $v = 2\pi$ (or multiples of it). This fact can be observed in Fig. 6. The $v = 2\pi$ Poincaré surface of section of the perturbed system is shown in Fig. 6a with different initial conditions and parameters $K = 1$ and $e = \beta = 0.03$. In this graph, four centers appear labeled with letters A–D. As it is well known,

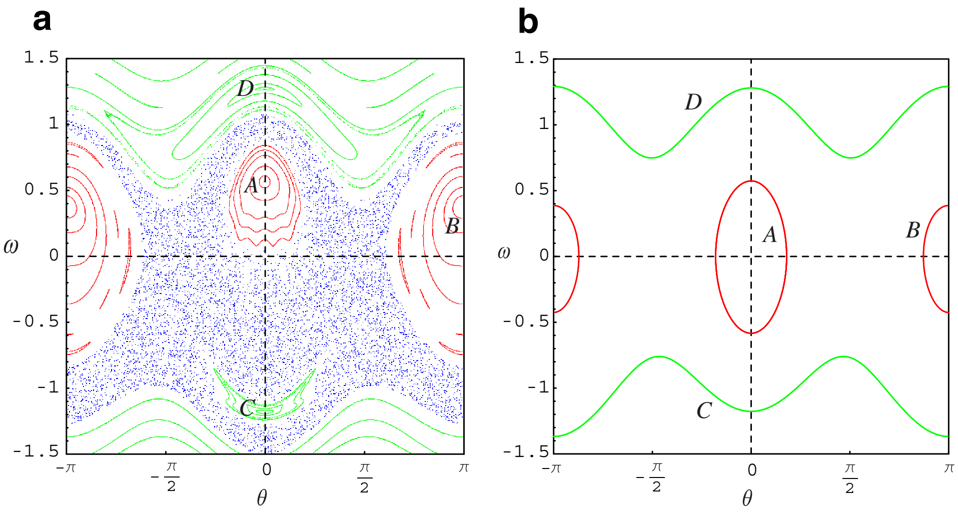

Fig. 6. (a) $v = 2\pi$ Poincaré surface of section of the perturbed spacecraft ($K = 1, e = \beta = 0.03$) with different initial conditions. (b) Trajectories in the reduced phase space of the 2π-periodic pitch motions corresponding to the centers labeled A–D.

these centers correspond to four different periodic pitch motions with the same period as the orbital motion, 2π. The trajectories of these 2π-periodic motions in the reduced phase space (θ, ω) can be seen in Fig. 6b. The motions A and B are periodic oscillations. In motion A, the positive z axis of the spacecraft is pointing towards Earth, whereas in oscillation B, the positive z axis is pointing outwards Earth. The motions C and D, are periodic tumbling rotations with opposite directions. Around the four centers of Fig. 6a there are closed curves which correspond to quasi-periodic motions. Finally, the big cloud of disordered points that fill the central part of this graph correspond to the chaotic pitch motions.

5. Control of the pitch motion with the ETDAS method

In this section a feedback method for controlling chaos is applied to the equations of motion (12) of the perturbed spacecraft in order to transform the chaotic pitch motions into one of those persistent 2π-periodic motions we have mentioned in the previous section. The particular feedback control method that we use in this section is the so-called extended time-delay autosynchronization or ETDAS. This method is a natural extension of the time-delay autosynchronization or TDAS technique [48]. The ETDAS method was first proposed by Socolar et al. [52] to overcome the limitations of the TDAS technique in stabilizing periodic orbits. In this way, the ETDAS has been successfully applied in several systems were TDAS had previously failed [3,52,1,49]. The ETDAS method has two important advantages: it does not requires fast switching or sampling, nor does it needs a reference signal corresponding to the desired regular motion. It only requires the knowledge of the period of the desired periodic orbit.

The basic block diagram of the ETDAS control method is shown in Fig. 7. In the operation of this method, the control variable y is progressively delayed at the output by multiples of some amount of time τ. Then all these delayed control values $y(t - j\tau)$ are re-introduced into the system through the feedback control signal

$$F(t) = k\left[y(t) - (1 - R)\sum_{j=1}^{\infty} R^{j-1} y(t - j\tau)\right].$$

where $0 \leqslant R < 1$ and k are the two adjustable parameters of this control signal.

When applied to periodic motion the delay time τ coincides with the period of the motion. In this way, the ETDAS method uses information of many previous states of the system in order to get the stabilization of the periodic orbit with period τ. It is worth to emphasize that for any values of the control parameters R and k, when the system follows a τ-periodic orbit, the control signal $F(t)$ vanishes, because in that case, $y(t - j\tau) = y(t)$ for all j (the identity

$$\frac{1}{1 - R} = \sum_{k=0}^{\infty} R^k$$

has to be taken into account).

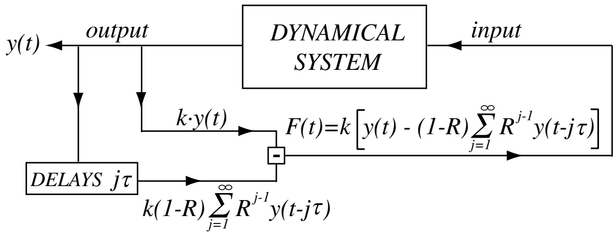

Fig. 7. Block diagram of the ETDAS control method.

Therefore, we assume that the perturbed spacecraft is acted upon additional forces, which introduce new terms in the equations of motion in order to control effectively the attitude dynamics of the spacecraft. To this end, we have applied the ETDAS method in such a way that the equations of motion of the perturbed spacecraft take the form

$$\begin{cases} \dot{\theta} = \omega, \\ \dot{\omega} = -K\sin\theta\cos\theta + Ke\cos v\sin\theta\cos\theta + 2e\sin v(\omega - 1) + \beta[\cos\theta\cos(v+\Omega) - 2\sin\theta\sin(v+\Omega)] + F(v), \end{cases} \tag{18}$$

where the feedback control signal $F(v)$ is given by

$$F(v) = k\left[\omega(v) - (1-R)\sum_{j=1}^{\infty} R^{j-1}\omega(v - j\tau)\right].$$

Thus, we have chosen as control variable the angular velocity ω. The delay time τ must be precisely the period of the persistent periodic pitch motions in the uncontrolled spacecraft, that is, the orbital period $\tau = 2\pi$. In this way, we have two different adjustable control parameters, k and $0 \leqslant R < 1$ in the added control term to get the control over the pitch motions of the spacecraft.

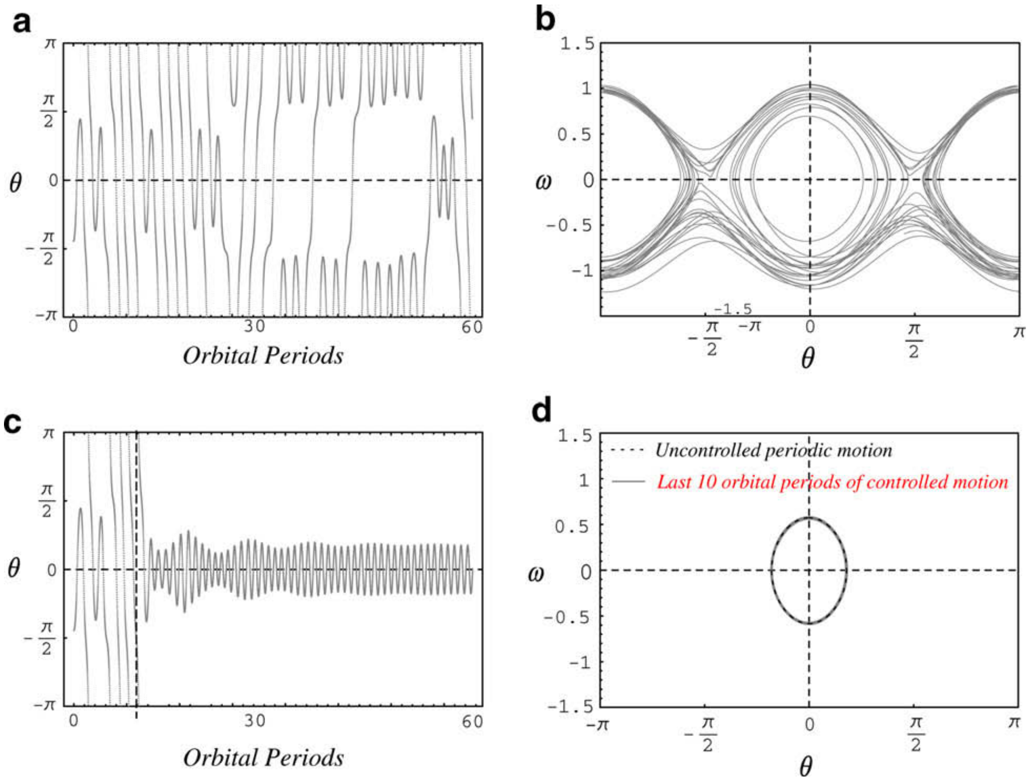

Fig. 8. An example of the success of the ETDAS control method for the case $(\theta_o, \omega_o) = (-1.4, 0)$ and $K = 1, e = \beta = 0.03$. Time history of θ angle (a) and trajectory in phase space (b) for the uncontrolled spacecraft. The same for the controlled spacecraft with control parameters $k = -0.1$, $R = 0.1$ in (c) and (d).

It is worth to point out that, when the controlled spacecraft follows a 2π-periodic motion, the control signal F vanishes. Thus, any 2π-periodic motion of the uncontrolled system (12) is also a 2π-periodic libration of the controlled spacecraft (18). As a consequence, when the system moves in the neighborhoods of the 2π-periodic motion we should

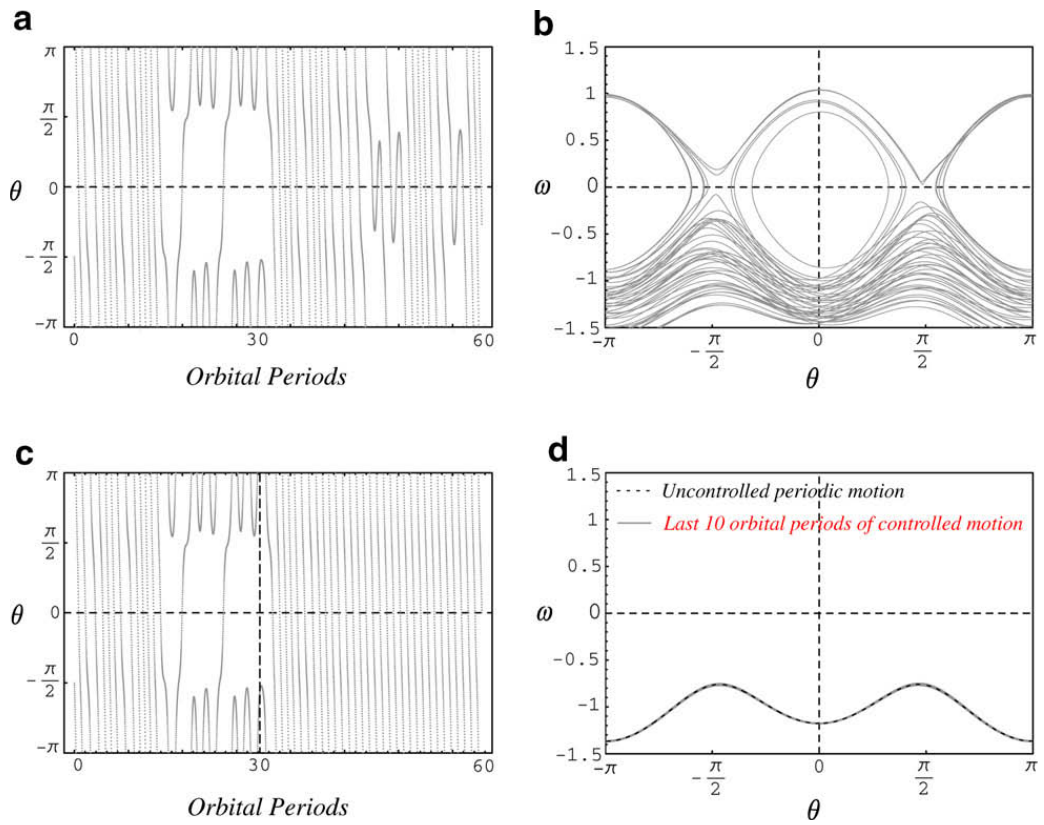

Fig. 9. Another example of the success of the ETDAS control method for the same parameters as Fig. 8 but different initial conditions $(\theta_o, \omega_o) = (-\pi/2, -0.9)$.

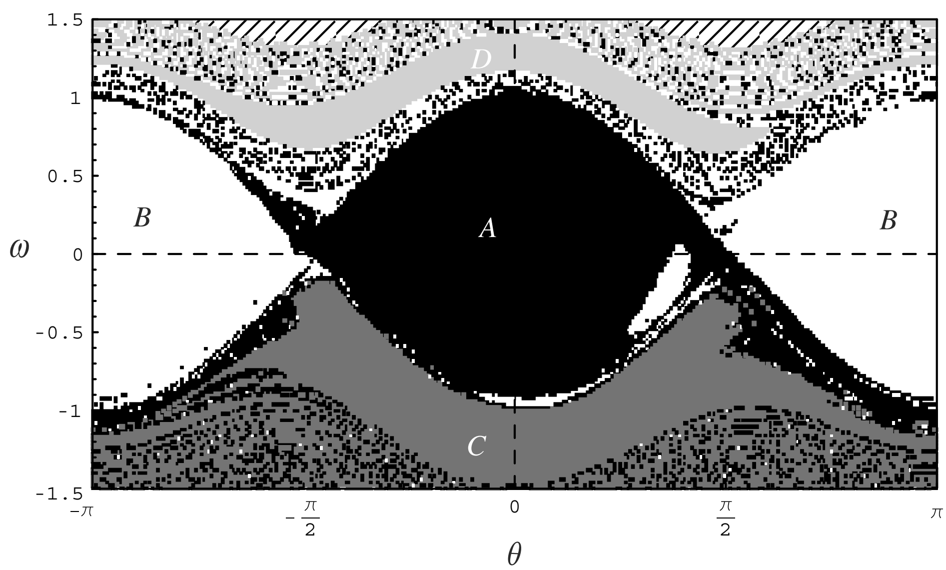

Fig. 10. Attraction basins of the 2π-periodic motions for the controlled spacecraft with $K = 1$, $e = \beta = 0.03$ and $k = -0.1$, $R = 0.5$. Black color stands for initial conditions tending to periodic motion A (Fig. 6). White color – periodic motion B. Dark grey color – periodic motion C. Clear grey color – periodic motion D. Striped areas – other periodic motions.

expect small values for the controlling force F (in fact, it is a torque acting on the spacecraft center of mass). Therefore, if this control method is successful, and if from the very beginning the spacecraft is moving close to one of those persistent periodic pitch motions, it can be controlled with small controlling forces. This is an attractive feature of this control method.

Fig. 8 shows an example of the tests we have carried out integrating numerically the equations of motion (18) of the controlled spacecraft. This example corresponds to a pitch motion with initial conditions $(\theta_o, \omega_o) = (-1.4, 0)$, and system parameters $K = 1$, $e = \beta = 0.03$, which are the same of Fig. 6. The upper graphs of this figure show the time history of the pitch angle θ (a), and the trajectory in phase space (b) for the uncontrolled spacecraft. The lower graphs show the same for the controlled spacecraft with control parameters $k = -0.1$, $R = 0.1$. The dashed vertical line in (c) indicates the moment when the control method is switched on. As it can be seen in figures (c) and (d), the control method succeeds transforming the initially chaotic pitch motion into a periodic oscillation of relatively small amplitude. In figure (d) it is depicted the controlled trajectory during only the last ten orbital periods. As it can be observed, it practically coincides with the persistent 2π-periodic oscillation of the uncontrolled spacecraft (black dashed line) which corresponds to the trajectory labeled A in Fig. 6b.

In Fig. 9 we show another example of control test for the same values of the system and control parameters, but different initial conditions $(\theta_o, \omega_o) = (-\pi/2, -0.9)$. As it can be seen in the graphs of this figure, the control method succeeds again, but now it transforms the initially chaotic pitch motion into a different 2π-periodic motion from the one of the previous example. In this case, the final periodic motion is not an oscillation but a tumbling rotation which correspond to the persistent periodic rotation of the uncontrolled spacecraft labeled C in Fig. 6b.

As these two examples of control shown in Figs. 8 and 9 point out, when the control method is applied to different initial conditions, not always it transforms the corresponding chaotic pitch motions into the same final periodic motion. Therefore, in order to get a global view of the effect of the control method on the system, we have focused on the geometry of the attraction basins of the four different persistent 2π-periodic motions of the uncontrolled spacecraft, when the control method is applied to it. To this end, a two-dimensional grid of initial conditions (θ, ω) with steps of 0.02, has been considered with fixed values of the system and control parameters. The controlled trajectories corresponding to each one of these initial conditions have been calculated integrating numerically the controlled equations of motion (18) in order to know its w-limit periodic trajectory. This grid is transformed into a matrix with different values depending on the corresponding w-limit periodic motion of each initial conditions. The resulting matrix is then submitted as input to the commercial software TRANSFORM [10] which produces the pictures as the one in Fig. 10 by assigning the same colors to the same values of the matrix.

Fig. 10 shows an example of the attraction basins of the different final periodic pitch motion for $K = 1$, $e = \beta = 0.03$ and $k = -0.1$, $R = 0.5$. Black color stands for those initial conditions whose controlled trajectories tend to the periodic oscillation labeled A in Fig. 6b. White color stands for those ones tending to the periodic oscillation labeled B in the same figure. Dark grey color stands for those ones tending to the periodic rotation labeled C. Clear grey color stands for those ones tending to the periodic rotation labeled D. Finally, the upper striped areas contain those ones tending to other different periodic motions. It is worth to note that, as it can be observed in Fig. 10, not only there are areas where the limits of the attraction basins are not well defined, but also many other areas where the attraction basins are completely mixed each other. We think that this fact means that although the perturbed system is under a control method, it has not lost its strong chaotic character, as it is still present the sensible dependence on initial conditions. Indeed, although two different initial conditions are very close together inside one of these mixing areas, it can be that their corresponding controlled trajectories tend to very different final periodic pitch motions.

6. Conclusions

The pitch attitude dynamics of an asymmetric magnetic spacecraft in a polar almost circular orbit subject to the influence of a gravity gradient torque has been studied. The system is perturbed by the small eccentricity of the elliptic orbit and by a small magnetic torque generated by the interaction between the Earth's magnetic field and the magnetic moment of the spacecraft. The geomagnetic field is modeled as a dipole aligned with the rotation axis of the Earth.

We have analytically established by means of the Melnikov method that both perturbations generate heteroclinic chaotic behavior in the pitch motion of the spacecraft. In addition, we have also investigated numerically the pitch attitude dynamics by using several tools based on computer simulations, including time history, Poincaré map and power spectrum. The analytical result given by the Melnikov method have been confirmed by this numerical research. Despite of the generation of chaos by the perturbations, we have also found in these numerical studies the persistency of some periodic pitch motions in the perturbed system with the same period as the orbital motion of the spacecraft.

In order to remove the chaotic motion generated by the perturbations, we have investigated the application of a feedback method for controlling chaos, the so-called extended time-delay autosynchronization or ETDAS. This control technique has two important advantages: it neither requires rapid switching or sampling, nor needs any reference signal corresponding to the desired periodic orbit, but only the period of it. By means of numerical simulations of the pitch motion of the controlled spacecraft, we have found that the ETDAS method succeeds being able to convert the initially chaotic pitch motions into those persistent periodic motion of the perturbed system.

Finally, with the goal of getting a global view of the effect of this control method on the attitude dynamics, we have calculated the attraction basins of the persistent 2π-periodic motions when the control method is applied. The study of the geometry of the attraction basins has revealed us that, despite of the control, the system has not lost completely its chaotic features, as it is present a sensible dependence on initial conditions with respect to the final periodic motions of the controlled attitude trajectories.

Acknowledgements

This work is included in the framework of the research project MTM2005-08595 supported by the Spanish Ministry of Education and Science.

References

[1] Batlle C, Fossas E, Olivar G. Extended time-delay autosynchronization of the buck converter, electronically available at http://arxiv.org/abs/chao-dyn/9609009.
[2] Beletsky VV, Lopes RVF, Pivovarov ML. Chaos in spacecraft attitude motion in Earth's magnetic field. Chaos 1999;9:493–8.
[3] Bleich ME, Socolar JES. Stability of periodic orbits controlled by time-delay feedback. Phys Lett A 1996;210:87–94.
[4] Boccaletti S, Grebobi C, Lai YC, Mancini H, Maza D. The control of chaos: theory and applications. Phys Rep 2000;329:103–97.
[5] Bryson AE. Control of spacecraft and aircraft. Princeton: Princeton University Press; 1994.
[6] Chen M, Zhou D, Shang Y. A simple time-delayed method to control chaotic systems. Chaos, Solitons & Fractals 2004;22:1117–25.
[7] El-Gohary A, Youssif YG. Optimal stabilization of the equilibrium positions of a rigid body using rotors. Chaos, Solitons & Fractals 2001;12:2007–14.
[8] El-Gohary A. Optimal stabilization of an equilibrium position of a rigid body using rotors system with friction forces. Chaos, Solitons & Fractals 2005;23:1585–97.
[9] Enns RH, McGuire GC. Nonlinear physics with mathematica for scientists and engineers. Boston: Birkhäuser; 2001.
[10] Fortner Research LLC. TRANSFORM, Sterling; 1996.
[11] Fujii HA, Ichiki W. Nonlinear dynamics of the tethered subsatellite system in the station keeping phase. J Guid Contr Dyn 1997;20:403–6.
[12] Fujii HA, Ichiki W, Suda SI, Watanabe TR. Chaos analysis on librational control of gravity-gradient satellite in elliptic orbit. J Guid Contr Dyn 2000;23:145–6.
[13] Ge ZM, Lee CI, Chen HH, Lee SC. Non-linear dynamics and chaos control of a damped satellite with partially-filled liquid. J Sound Vib 1998;217:807–25.
[14] Goldstein H, Poole CP, Safko JL. Classical mechanics. 3rd ed. Upper Saddle River: Pearson; 2001.
[15] Gradshteyn IS, Ryzhik IM. Table of integrals, series and products. San Diego: Academic Press; 1980.
[16] Gray GL, Kammer DC, Dobson I, Miller AJ. Heteroclinic bifurcations in rigid bodies containing internally moving parts and a viscous damper. J Appl Mech Trans ASME 1999;66:720–8.
[17] Guckenheimer J, Holmes P. Nonlinear oscillations, dynamical systems and bifurcations of vector fields. New York: Springer-Verlag; 1983.
[18] Hale FJ. Introduction to space flight. Englewood Cliffs: Prentice-Hall; 1994.
[19] Holmes PJ, Marsden JE. Horseshoes and Arnold diffusion for Hamiltonian systems on Lie groups. Indiana Univ Math J 1983;32:273–309.
[20] Hughes PC. Spacecraft attitude dynamics. New York: John Wiley & Sons; 1986.
[21] Iñarrea M, Lanchares V. Chaos in the reorientation process of a dual-spin spacecraft with time-dependent moments of inertia. Int J Bifurc Chaos 2000;10:997–1018.
[22] Iñarrea M, Lanchares V, Rothos VM, Salas JP. Chaotic rotations of an asymmetric body with time-dependent moments of inertia and viscous drag. Int J Bifurc Chaos 2003;13:393–409.
[23] Iñarrea M, Lanchares V. Chaotic pitch motion of an asymmetric non-rigid spacecraft with viscous drag in circular orbit. Int J Non-Linear Mech 2006;41:86–100.
[24] Iñarrea M, Peláez J. Libration control of electrodynamic tethers using the extended time-delayed autosynchronization method. Adv Astronaut Sci 2007;127:1393–408.

[25] Ji JC, Hansen CH. Stability and dynamics of a controlled van der Pol-Duffing oscillator. Chaos, Solitons & Fractals 2006;28:555–70.
[26] Karasopoulos HA, Richardson DL. Chaos in pitch equation of motion for the gravity-gradient satellite. AIAA; 1992. paper 92-4369.
[27] Karasopoulos HA, Richardson DL. Numerical investigations of chaos in the attitude motion of a gravity-gradient satellite. American Astronomical Society; 1993. p. 93–581.
[28] Klemperer WB, Baker Jr RM. Satellite libration. Astronaut Acta 1956;3:16–27.
[29] Klemperer WB. Satellite librations of large amplitude. ARS J 1960;30:123–4.
[30] Koiller J. A mechanical system with a "wild" horseshoe. J Math Phys 1984;25:1599–604.
[31] Korte M, Constable CG. The geomagnetic dipole moment over the last 7000 years–new results from a global model. Earth Planet Sci Lett 2005;236:348–58.
[32] Lambert JD. Computational methods in ordinary differential equations. London: John Wiley & Sons; 1976.
[33] Lanchares V, Iñarrea M, Salas JP. Spin rotor stabilization of a dual–spin spacecraft with time dependent moments of inertia. Int J Bifurc Chaos 1998;8:609–17.
[34] Liu CL, Tian YP. Eliminating oscillations in the Internet by time-delayed feedback control. Chaos, Solitons & Fractals2008; 35(5):878–887
[35] Meehan PA, Asokanthan SF. Chaotic motion in a spinning spacecraft with circumferential nutational damper. Nonlinear Dyn 1997;12:69–87.
[36] Meehan PA, Asokanthan SF. Control of chaotic instabilities in a spinning spacecraft with dissipation using Lyapunov's method. Chaos, Solitons & Fractals 2002;13:1857–69.
[37] Melnikov VK. On the stability of the center for time periodic perturbations. Trans Moscow Math Soc 1963;12:1–56.
[38] Modi JV, Brereton RC. Periodic solutions associated with the gravity-gradient-oriented system: Part I. Analytical and numerical determination. AIAA J 1969;7:1217–25.
[39] Modi JV, Brereton RC. Periodic solutions associated with the gravity-gradient-oriented system: Part II. Stability analysis. AIAA J 1969;7:1465–8.
[40] Moran JP. Effect of plane librations on the orbital motion of a Dumbell satellite. ARS J 1961;31:1089–96.
[41] NASA SP-8018. Spacecraft magnetic torques; 1969.
[42] NASA SP-8024. Spacecraft gravitational torques; 1969.
[43] NASA SP-8058. Spacecraft aerodynamic torques; 1971.
[44] Nixon MS, Misra AK. Nonlinear dynamics and chaos of two body tethered satellite systems. American Astronomical Society; 1993. p. 93–731.
[45] Nusse HE, Yorke JA. Dynamics numerical explorations. 2nd ed. New York: Springer; 1998.
[46] Peláez J, Lorenzini EC. Libration control of electrodynamic tethers in inclined orbit. J Guid Contr Dyn 2005;28:269–79.
[47] Peng J, Liu Y. Chaotic motion of a gyrostat with asymmetric rotor. Int J Non-Linear Mech 2000;35:431–7.
[48] Pyragas K. Continuous control of chaos by self–controlling feedback. Phys Lett A 1992;170:421–8.
[49] Pyragas K. Control of Chaos via extended delay feedback. Phys Lett A 1995;206:323–30.
[50] Schindler GM. On satellite librations. ARS J 1959;29:368–70.
[51] Sidi MJ. Spacecraft dynamics and control. New York: Cambridge University Press; 1997.
[52] Socolar JES, Sukow DW, Gauthier DJ. Stabilizing unstable periodic orbits in fast dynamical systems. Phys Rev E 1994;50:3245–8.
[53] Song Y, Wei J. Bifurcation analysis for Chen's system with delayed feedback and its application to control of chaos. Chaos, Solitons & Fractals 2004;22:75–91.
[54] Tam PT. A physicist's guide to mathematica. San Diego: Academic Press; 1997.
[55] Teofilatto P, Graziani F. On librational motion of spacecraft. Chaos, Solitons & Fractals 1996;7:1721–44.
[56] Tong X, Rimrott FPJ. Numerical studies on chaotic planar motion of satellites in an elliptic orbit. Chaos, Solitons & Fractals 1991;1:179–86.
[57] Tong X, Tabarrok B, Rimrott FPJ. Chaotic motion of an asymmetric gyrostat in the gravitation field. Int J Non-Linear Mech 1995;30:191–203.
[58] Tsui APM, Jones AJ. The control of higher dimensional chaos: comparative results for the chaotic satellite attitude control problem. Physica D 2000;135:41–62.
[59] Wiesel WE. Spaceflight dynamics. 2nd ed. New York: McGraw-Hill; 1997.
[60] Wolfram S. The mathematica book. 4th ed. Cambridge: Cambridge University Press; 1999.